



# Numerical investigation of effect of Reynolds number and spin ratio on aerodynamic coefficients of Flettner rotor

Prasad Deshpande, Dr. D.K. Chavan

Research Scholar, Department of Mechanical Engineering, Shri Jagdishprasad Jhabarmal Tibrewala University, India  
Ex. Principal, Siddhant College of Engineering, Pune, India

**ABSTRACT:** Trepidation of the shipping industry today is not only to lower the cost of operation but also the carbon footprint. The Flettner rotor is inviting growing consideration as a possible technology for wind-assisted ship propulsion. Nevertheless, the impact of the Reynolds number on the aerodynamic performance of rotating cylinders is still imprecise. This study deals with numerical simulation on a large-scale Flettner rotor. The cylinder diameter,  $d = 1\text{m}$  and its height,  $H = 3.73\text{m}$ . The simulations are carried out at various spin ratios, ( $k$ ) ranging from 0 to 5 and at Reynolds number, ( $Re$ )  $1.8 \times 10^5$  to  $1 \times 10^6$ . The outcomes show that the lift coefficient is influenced by the Reynolds number in the critical flow region and when the spin ratio is less than 2.5, however Reynolds number influences the coefficient of drag for all flow conditions examined.

**KEYWORDS:** Flettner rotor, spinning cylinder, Magnus effect, wind assisted shipping

## SYMBOLS AND ABBREVIATIONS

$d$	Cylinder diameter	$m$
$H$	Cylinder height	$m$
$\Omega$	Angular velocity	$\text{rad/s}$
$V$	Tangential velocity	$\text{m/s}$
$\rho$	Density of air	$\text{kg/m}^3$
$\nu$	Kinematic viscosity of air	$\text{m}^2/\text{s}$
$U$	Free stream velocity	$\text{m/s}$
$AR$	Aspect ratio	$(H/d)$
$k$	Spin ratio	$V/U$
$A_s$	Surface area of cylinder	$\text{m}^2$
$F_D$	Drag force	$N$
$F_L$	Lift force	$N$
$Re$	Reynolds number	$(U \times d)/\nu$
$C_D$	Coefficient of drag,	$F_D / (0.5 \times \rho \times U^2 \times H \times d)$
$C_L$	Coefficient of lift,	$F_L / (0.5 \times \rho \times U^2 \times H \times d)$
$CP$	Coefficient of pressure,	$\text{Pressure} / (0.5 \times \rho \times U^2)$

## I. INTRODUCTION

A large part of the cost of operating a ship is its fuel cost. As environmental directives [1], get more critical, improving fuel efficiency is the prudent way to successfully regulate operating costs. Until the late 19th century, wind was the major power source for ships. When wind is complimentary, sails can be used to reduce necessary power input in wind-assisted ships (WAS), which primarily use engine for propulsion. Kites and Flettner rotors are potent technologies exploiting wind energy for ship propulsion. The Flettner rotor is a spinning cylinder which produces an aerodynamic lift owing to the Magnus effect. The Flettner rotor is gaining more and more attention as a feasible technology for wind assisted ship propulsion. Even though the proven model, the rotor ship was forsaken since it could not contend with the swelling



acceptance of diesel engines and with the low oil price then. Since its initiation, the Flettner rotor was rarely used for pragmatic applications in the maritime field, however, the physical marvels associated with spinning cylinders, fascinated many scientists for years. Recently, however, the prospect of using wind energy as a supplementary form of propulsion for ships has once more turned out to be of importance due to the unpredictable fuel prices and the tough environmental protocols. [2], is involved in special projects at ENERCON has said that the use of the Flettner- rotors will allow for savings up to 15% and this savings can be significantly more in good wind conditions.

In the mid 1920's, an effort to produce energy from the 'Magnus Effect' from spinning cylinders was made by Anton Flettner. He proved the usefulness of the concept by substituting the sails by spinning cylinders for the propulsion of big ships, through the alteration of the 'Buckau' and 'Barbara'. [3], was the first to carry out methodical study on the Flettner rotor at the Langley Field NACA Laboratory. He employed Reynolds number ranging between  $3.9 \times 10^4$  to  $1.1 \times 10^5$  for spinning cylinder of aspect ratio 13, without endplates. The results show that for the considered range, the Reynolds number has an insignificant effect on both the lift and drag coefficients. [4], used disc at the ends of the spinning cylinder and demonstrated that the use of such discs decreases induced drag. [5], applied the Kutta-Joukowski theory to the study of the Flettner rotor ship. The work of [6], is a significant input in the study of Flettner rotors. Thom carried out a number of force and pressure measurements of spinning cylinders, to study the impact of aspect ratio, surface roughness and endplates on the aerodynamic forces. The experiments were carried out on spinning cylinder of aspect ratio 12.5 subjected to flow having Reynolds number in the range of  $5.3 \times 10^4$  to  $8.8 \times 10^4$ . The results show that for the considered range, the Reynolds number has an insignificant effect on both the lift and drag coefficients. Quite a few years later [7], came up with a comprehensive precis of the experiments on spinning cylinders done till then. Findings of a set of two-dimensional tests carried out by Swanson in the Reynolds number range  $3.5 \times 10^4$  to  $5.0 \times 10^5$  for spin ratios from 0 to 1 were also stated. A notable product of this study is that, for spin ratio less than 0.5 and Reynolds number in the range of  $1.3 \times 10^5$  to  $5.0 \times 10^5$ , the lift coefficient turns out to be negative and the drag coefficient looks to be significantly affected by the change of the Reynolds number up to spin ratio 0.75. [8], did experiments at two dissimilar Reynolds numbers, viz.  $1.7 \times 10^4$  and  $4.9 \times 10^4$ , on a spinning cylinder of aspect ratio 10.4 fitted with endplates of size 1.4 times the diameter of the cylinder and two times the diameter of the cylinder. The investigation shows that when the bigger endplate size is used the outcome is indifferent to the Reynolds numbers contemplated. However, for the smaller sized endplate, Clayton, deduced that a lower Reynolds number results in a decrease in the lift coefficient and rise in drag coefficient. This outcome is observed until spin ratio,  $k = 2$ . [9], has said that surface roughness of a rotor has some influence on lift and that at least one experiment has showed that rough cylinders offer minimum 30% more lift as compared to smooth cylinders at low Reynolds numbers. [10], finished a sequence of trails on a spinning cylinder, with no endplates and having aspect ratio 18.7. The Reynolds number employed was  $3.8 \times 10^3$ . They state that, for low spin ratios, their outcomes overestimate the lift coefficient in comparison with the one reported by [3]. [11], have experimentally investigated the effects of endplates on the aerodynamic behaviour of a spinning cylinder in crossflow. The finest development in lift performance was realized with two identical sized plates that spin with the cylinder. [12], conducted a series of trails on a cylinder of aspect ratio 5.1 with no endplates. The Reynolds numbers ranged between  $1.9 \times 10^4$  and  $9.6 \times 10^4$ . [13], carried out wind-tunnel experiments on a spinning cylinder for a Reynolds number  $4.0 \times 10^4$ . The aspect ratio of the cylinder was 6. The outcome shows comparable findings with that of [12]. [14], performed a series of wind tunnel experiments at Reynolds number ranging from  $1.8 \times 10^5$  to  $1 \times 10^6$  and at spin ratio 0 to 5. The authors conclude that there is notable impact of the Reynolds number on the drag and lift coefficients below spin ratio  $k = 2.5$ .

During the past few years, in addition to the experimental studies, many Computational Fluid Dynamics (CFD) simulations on the subject of spinning cylinders were also published. Two-dimensional flows at Reynolds number less than  $1.0 \times 10^3$  have been simulated by [15], [16] and [17]. [17], carried out simulations at Reynolds number = 200 and,  $k = 4$ . The findings show that coefficient of lift is approximately equal to 12 and the drag coefficient to be 0. [18], conducted Large Eddy Simulations on a cylinder at Reynolds number  $1.4 \times 10^5$  for spin ratio up to 2. In an earlier work by [19], it is stated that for Reynolds number between  $5.0 \times 10^4$  and  $1.0 \times 10^5$ , it is non influent if spin ratio is less than 2. [20], studied the consequence of spanwise discs on a spinning cylinder configuration for spin ratio in the range of 1.9 to 3.4. The findings show that in comparison with a configuration without spanwise discs, the streamwise component of velocity is improved between the boundary layer of two facing discs, mainly for spin ratio greater than 2.5. [21], also conducted two-dimensional CFD simulations on a spinning cylinder at Reynolds number  $5.0 \times 10^5$ ,  $1.0 \times 10^6$  and  $5.0 \times 10^6$  for spin ratio range 2 to 8. The findings show that the lift and drag coefficients are only slightly affected by the Reynolds number. [22], conducted CFD simulations for the same Reynolds numbers as [21]. The authors arrive at a conclusion that the Reynolds number has a noticeable impact on both the lift and drag coefficients. A rise in Reynolds number yields a high rise in lift coefficient and a drop in drag coefficient. [23], carried out CFD simulations at Reynolds number  $5.11 \times 10^6$  of a spinning cylinder of aspect ratio 3.5, with and without endplates. The authors accept that data is

fairly distributed and not dependable for performance predictions. [24], made numerical models of a Flettner rotor and a towing kite. The authors computed wind-generated thrust and propulsive power and its dependency on the local wind and ship speed. They suggest that average wind power contribution for a single Flettner rotor ranges between 193 kW and 373 kW.

The review presented here shows that, in spite of the many publications, the effect of the Reynolds number on the aerodynamic coefficients of a spinning cylinder still needs to be further analyzed. This is owing to two key reasons. The first reason being that, maximum of the existing experimental data was found at subcritical or lower Reynolds numbers. [7], conducted experiments at higher Reynolds numbers but, the spin ratio was restricted to  $k = 1$ . Only recently [14], performed a series of wind tunnel experiments at Reynolds number ranging from  $1.8 \times 10^5$  to  $1 \times 10^6$  but even they have not conducted experiments for higher spin ratios for all the Reynolds number. The second reason is that, though the CFD investigations were extended to the supercritical regime but the findings of different authors are contradictory to each other. The spin ratio, and the aspect ratio, are parameters that were tested to make an impact on aerodynamic performance of a Flettner rotor. The effect of the Reynolds number is still a matter of deliberation as it is seen from the studies done on this topic till date.

In this study, 3D numerical investigations have been carried out for combination of various Reynolds numbers and for different spin ratios. The division of the Magnus force can be done as a lift force and drag force. The component perpendicular to the free stream velocity is called the lift force and the component parallel to the flow is called the drag force. The flow conditions are chosen such that the influence of the critical and supercritical Reynolds number on the coefficient of lift and drag over the entire range is analyzed.

## II. EXPERIMENTAL WORK AND VALIDATION OF NUMERICAL RESULTS WITH EXPERIMENTAL RESULTS

[14], carried out wind tunnel experiments on spinning cylinder at critical and supercritical Reynolds number. Simulation for combination of various Reynolds numbers and for different spin ratios have been carried out in this study. The numerical setup offered here has been compared with the experimental setup of [14]. [14], used the boundary-layer test section of Politecnico di Milano wind tunnel to carry out the experiments. The test section is 13.84m in width, 3.84m in height and 35m in length. The cylinder was placed at the centre of the test section. As shown in (Fig.1), spinning cylinder with 1m diameter and 3.73m height was used. Lift, drag and torque were measured using the three-component force balance. Use of two different systems for pressure measurement, viz. one high sample-rate pressure scanner (PSI ESP-32HD) and one AMS 4711 was done. Analysis for uncertainty in measurement was carried out and the authors achieved a 95% uncertainty confidence level. For the measurement of the actual pressure on the outer skin of the cylinder, the static pressure inside the cylinder was also measured. A pressure tube was used for this measurement. The turbulent intensity of this test section is 2% while the thickness of the boundary layer is about 0.2 m. A pitot tube was positioned 5m in front of the cylinder and 1.85m above the ground. This pitot tube served in measuring the flow velocity.

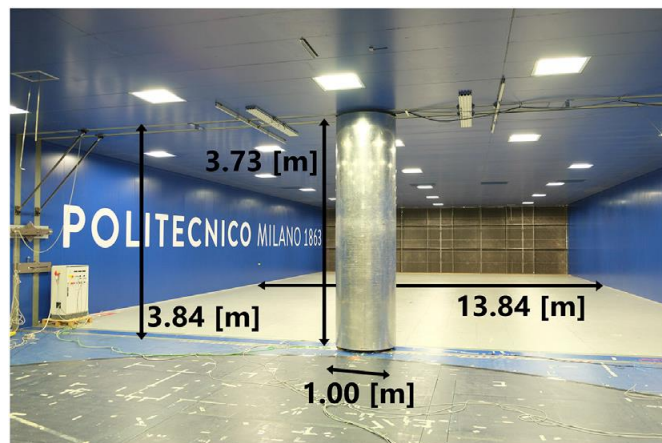


**Fig. 1. The Delft Rotor in Politecnico di Milano wind tunnel. [14]**

### A. NUMERICAL METHOD

The vital laws that rule the mechanics of fluids are the conservation of mass or the continuity equation, linear momentum and energy. All fluid motions where the continuum approximation is valid are governed by the continuity and momentum equation. For single phase and for a finite control volume these can be written as equations 1, 2 and 3 given below.

Continuity equation:

$$\frac{d}{dt} \int_V \rho dV + \oint_A \rho \mathbf{v} \cdot d\mathbf{a} = \int_V S_u dV \quad (1)$$

Momentum equation:

$$\frac{d}{dt} \int_V \rho \mathbf{v} dV + \oint_A \rho \mathbf{v} \otimes \mathbf{v} \cdot d\mathbf{a} = - \oint_A p \mathbf{I} \cdot d\mathbf{a} + \oint_A \mathbf{T} \cdot d\mathbf{a} + \int_V \mathbf{f}_b dV \quad (2)$$

Energy equation:

$$\frac{d}{dt} \int_V \rho E dV + \oint_A \rho H \mathbf{v} \cdot d\mathbf{a} = - \oint_A \dot{q}'' \cdot d\mathbf{a} + \oint_A \mathbf{T} \cdot \mathbf{v} \cdot d\mathbf{a} + \int_V S_E dV \quad (3)$$

In STAR-CCM+, these conservation laws are integrated over all the control volumes. These integral equations are then transformed to algebraic equations, by generating a set of approximations for the terms in the integral equations. The SST k- $\omega$  turbulence model [25], is a eddy-viscosity model of two-equation. The shear stress transport (SST) formulation gives us advantages of two different things. The use of a k- $\omega$  formulation in the inner parts of the boundary layer makes the model directly usable all the way down to the wall through the viscous sub-layer, hence the SST k- $\omega$  model can be used as a Low-Re turbulence model without any extra damping functions. The SST formulation also switches to a k- $\epsilon$  behaviour in the free-stream and thereby avoids the common k- $\omega$  problem that the model is too sensitive to the inlet free-stream turbulence properties. The SST k- $\omega$  model offers good behaviour in adverse pressure gradients and separating flow. The SST k- $\omega$  model produces large turbulence levels in regions with large normal strain, like stagnation regions and regions with strong acceleration. This tendency is much less pronounced than with a normal k- $\epsilon$  model though. Since algebraic equations are being resolved, the solutions found will not completely satisfy the laws of conservation after one iteration. Therefore, it is important to iterate repeatedly within each time step. A factor that is indicative of the convergence of a solution is the residuals, which shows the deviation of the algebraic solution. Usually, if the residuals of these continuity equations approach zero, this means the solution is converging. However, this may not be enough. The time discretization used is implicit, as this gives us more liberty in choosing the mesh size with no restraint forced by the numerical scheme. The analysis is unsteady and the time step is specified by using one degree of rotation of the cylinder per time step.

### B. NUMERICAL SETUP

The simulations are carried out to assess the effect of measurable factors like Reynolds number and spin ratio on the behavioural responsiveness of Flettner rotors. In the ensuing, the numerical setup is introduced. Cylinder diameter,  $d = 1\text{m}$  and its height,  $H = 3.73\text{m}$  corresponding to an aspect ratio,  $AR = 3.73$  is chosen for the simulations to be performed. In this study, Unsteady Reynolds Averaged Navier-Stokes (U-RANS) simulations are performed using simulation software Simcenter STAR-CCM+ v 13.06.012 for preparatory design of Flettner rotor as supplementary propulsion device. As a first step towards discretization implicit unsteady finite volume method is the selected algorithm and segregated flow is used with second order discretization for all convective terms. The segregated solver is invoked by the segregated flow model. The segregated flow solver solves each of the momentum equations in turn, one for each dimension. The linkage between the momentum and continuity equations is achieved with a SIMPLE predictor-corrector approach. A rectangular box-shaped domain is designed around the spinning cylinder (Fig. 2). The regions segment in STAR-CCM+ is used to select the boundaries of the computational domain.

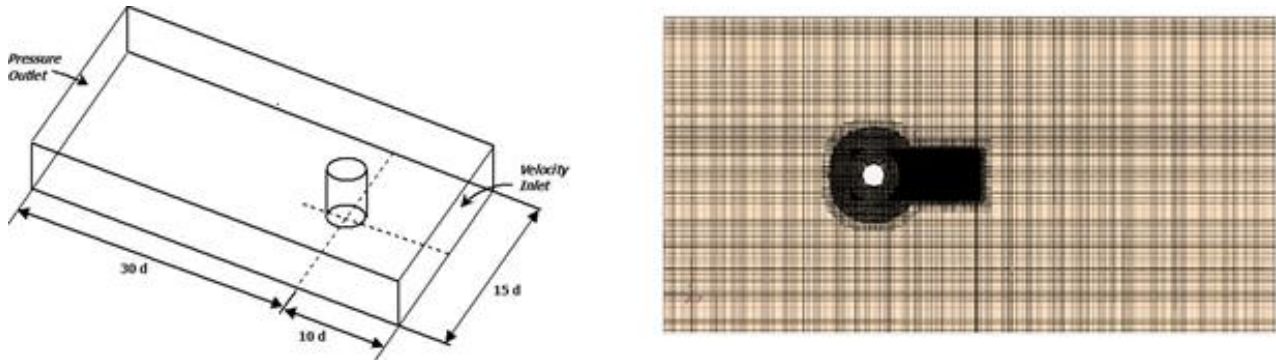


**Fig.2 Sectional top view of the mesh and simulation domain with boundary conditions**

Different boundary conditions are selected for every parameter. The front side of the domain has been set as a velocity inlet boundary condition with a recommended velocity. This inlet velocity also has been used to determine the spin ratio of the rotor spinning at an angular speed  $\Omega$ . A pressure outlet boundary condition with a relative pressure of value 0 Pa has been laid down on the rear side of the domain surface. No slip wall boundary condition is set on the opposite side of the domain. The top and bottom of the domain are set as symmetry planes. No slip wall is also used to define the cylinder boundary condition. In the calculations the flow is assumed to be incompressible. To take into account the effect of boundary layer, two layer all  $y^+$  wall treatment is efficiently utilized. The height of the first mesh cell of the cylinder wall is computed using flat plate boundary layer theory to achieve a desired  $y^+$  value of 1. The calculations for this are done taking into account the freestream velocity, freestream density, dynamic viscosity and the reference length. Completely turbulent calculations are performed using the  $k-\omega$  Shear Stress-Transport (SST) turbulence model. [25], [26]. The turbulent intensity of the flow channel is assumed to be 2%. Additionally, the rotation of cylinder in the simulation is attained by overset mesh (chimera mesh) method with distance weighted interpolation. A cylindrical overlap area has been created around the cylinder. This overlap between the fixed domain and the rotating mesh is an essential condition for putting to use the overset mesh method. The mesh used is trimmed cell type. This type is useful in modelling external aerodynamic flows owing to its capability to refine cell in wake region. Table.1 gives some more details of the physics values used in these simulations.

**Table 1 Physics values**

Space	Three Dimensional	
Time	Implicit unsteady	
Flow	Segregated Flow	
Equation Of state	Constant Density	
Viscous Regime	Turbulent	
Reynolds-Averaged Turbulence	K-Omega Turbulence	
Node	Property	Setting
Segregated flow>Velocity	Under Relaxation Factor	0.5
Segregated flow>Pressure	Under Relaxation Factor	0.5
Stopping Criteria		
Maximum Physical Time	Value	10 - 60 s
Maximum Inner Iterations	Value	5

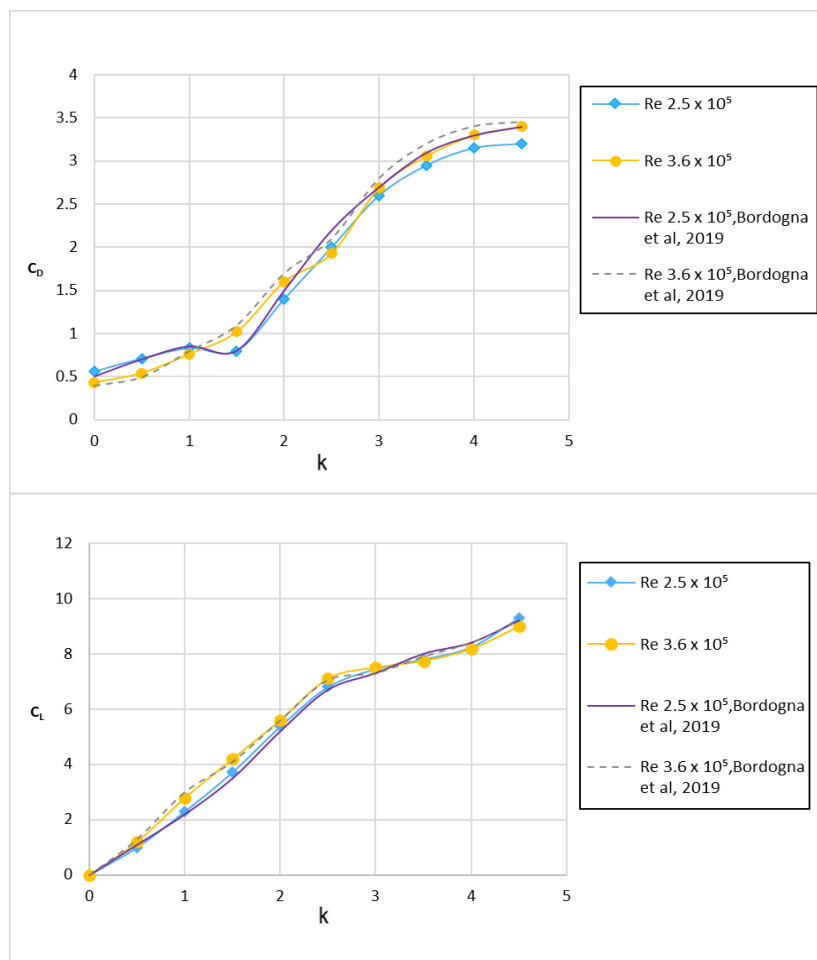
In order to carry out the grid dependency study different base sizes of 0.75m, 0.5m, 0.25m, 0.2m have been used. The base size of 0.5m which is a good compromise between speed and accuracy of the calculations is finally chosen for all the simulations. Computing facilities at the Tolani Maritime Institute have been used for the simulations performed.

### C. AUGMENTATIONS OVER EXPERIMENTAL INVESTIGATION USING CFD

In these experiments done by Bordogna, et al., effects caused by the wind-tunnel walls were not measured. The pressure inside the spinning cylinder could not be measured for some Reynolds number due to technical issues. Also, the calculations for the uncertainty relative to the measurements carried out for  $Re = 5.5 \times 10^5$  was not possible for [14], and the pressure coefficient curves are also not available for this Reynolds number. In the experimental investigation, by Bordogna, et al. the effect of wind-tunnel walls could not be measured also there were technical issues in the measurement of pressure inside the spinning cylinder. All of these problems are easily handled using CFD technique.

### D. VALIDATION OF NUMERICAL RESULTS WITH EXPERIMENTAL RESULTS

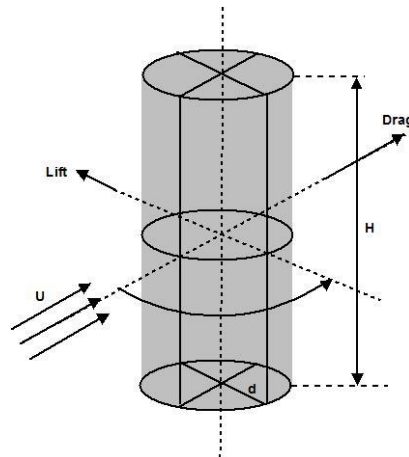
(Fig. 3) shows the comparison of the coefficient of lift and drag obtained from numerical study with experimental results studied at two different Reynolds number and for spin ratios ranging from 0 to 4.5. From the comparison made in (Fig. 3) it can be seen that the results of this study are in good agreement with the findings of [14], as similar aspect ratio and Reynolds number have been used in this study.



**Fig. 3 Comparison of numerical results with experimental results**

**III. RESULTS**

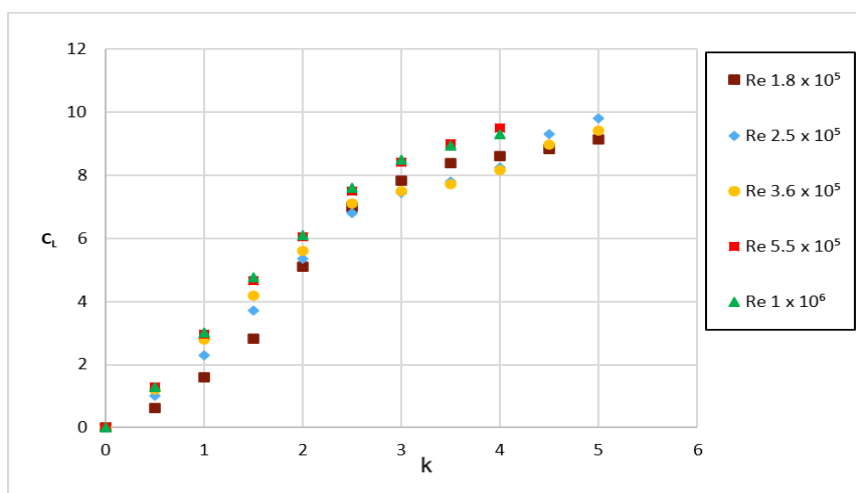
The influence of important factors on the aerodynamics of a Flettner rotor will be explained in this section. To understand the findings stated in the following sections, the direction of cylinder rotation and the conventions used in the current study are shown in (Fig. 4).

**Fig. 4 Main pertinent parameters of Flettner rotor**

The aerodynamic features of a Flettner rotor are mainly influenced by the spin ratio between the tangential speed of the rotor and the free stream velocity. [7], has found earlier that the coefficient of lift and drag of a spinning cylinder at low spin ratios,  $k < 1$  display a substantial reliance on Reynolds number. Similarly, [12], has confirmed that the lift and drag of a spinning cylinder at low spin ratios shows a substantial reliance on Reynolds number in terms of variation in lift.

**A. LIFT COEFFICIENT**

In this study the lift coefficients  $C_L$  (Fig. 5) seem to be affected by the Reynolds number. For the spin ratio in the range of  $k = 0$  to 2.5, higher Reynolds numbers give on to higher coefficients of lift. Further, for spin ratios  $k > 2.5$ , the lift coefficient does not look to be affected much by the Reynolds number. This is also reinforced by the reality that the impact of the Reynolds number on the lift coefficient seems to decrease with the increase of the spin ratio.

**Fig. 5 Overall lift co-efficient versus spin ratio**

Simulations on three-dimensional cylinders shorn of endplates, by [12], and [27], show that the lift coefficient stops to increase after a certain spin ratio and that this depends on the aspect ratio of the cylinder. In [23], study on a cylinder with an aspect ratio (AR = 3.5) similar as the one used in this study (AR = 3.73) is done at  $Re = 5.11 \times 10^6$ . The outcomes indicate that, for cylinder without endplates, the slope of the lift coefficient becomes constant at  $k = 2$  (Fig. 6). In this study, for the spin ratios considered, the lift coefficient slope does not become constant, and this is because the geometry chosen is pseudo two dimensional. Actually, the study of [27] and [13], suggests that the dissipation of the tip vortices circulation reduce the lift produced by the spinning cylinder. Additionally, for the aspect ratio AR = 3.5, the lift coefficient findings of the cylinder with endplates stated in [23], are more similar with the results of the current study. Though for a larger aspect ratio AR = 5.1, the findings of [12], regarding a spinning cylinder with two non-rotating endplates of size twice the diameter of the cylinder display a comparable trend to the findings of the lift coefficients found in the current study (Fig. 6). In the study of [12], the slope of the curve for coefficient of lift decreases at  $k = 2.5$  and the curve does not become constant till  $k = 5$ . In comparison with the current work, the coefficients of lift measured in [12], are much lower. It is acceptable as this is due to the significantly lower Reynolds number used.

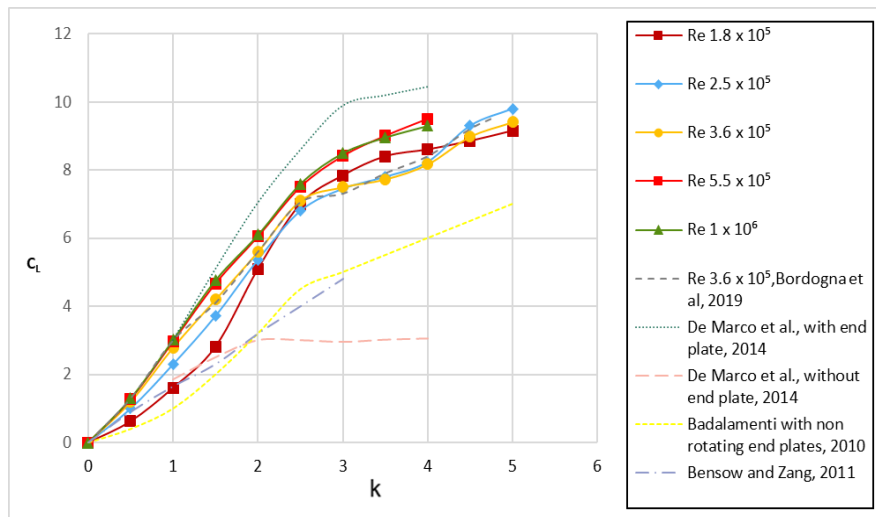


**Fig. 6 Comparison lift coefficient with other studies.**

**B. DRAG COEFFICIENT**

The overall coefficient of drag results are more dispersed (Fig. 7). The overall coefficient of lift results does not show such scatter, this is primarily because the coefficient of drag is influenced by even slight changes in pressure distribution. The obvious effect of Reynolds number for non-rotating cylinder is curbed by the rotation. At higher spin ratios, until  $k = 2.5$ , the Reynolds number shows a clear impact on the coefficient of drag, this is very comparable to the lift coefficient, a higher Reynolds number involves a higher coefficient of drag. However, the effect of Reynolds number is seen during the complete range of Reynolds number considered, this is very different from the coefficient of lift. For spin ratios greater than 2.5, the drag coefficients obtained for Reynolds number  $2.5 \times 10^5$  and  $3.6 \times 10^5$  don't display any notable difference. However, at  $k = 2$ , the variance between the coefficient of drag obtained at Reynolds number  $1.8 \times 10^5$  and  $5.5 \times 10^5$  is still significant.

[23], have expressed that, for cylinder without endplates, both the coefficient of lift and the coefficient of drag stop to increase at  $k = 2$  (Fig. 8). However, if the cylinder is having endplates, the coefficient of drag increases with increase in the spin ratio. Consequently [12], and [13], have shown that for spin ratios greater than 3, spinning endplates produce more drag than a cylinder devoid of endplates or cylinder with non-spinning endplates.

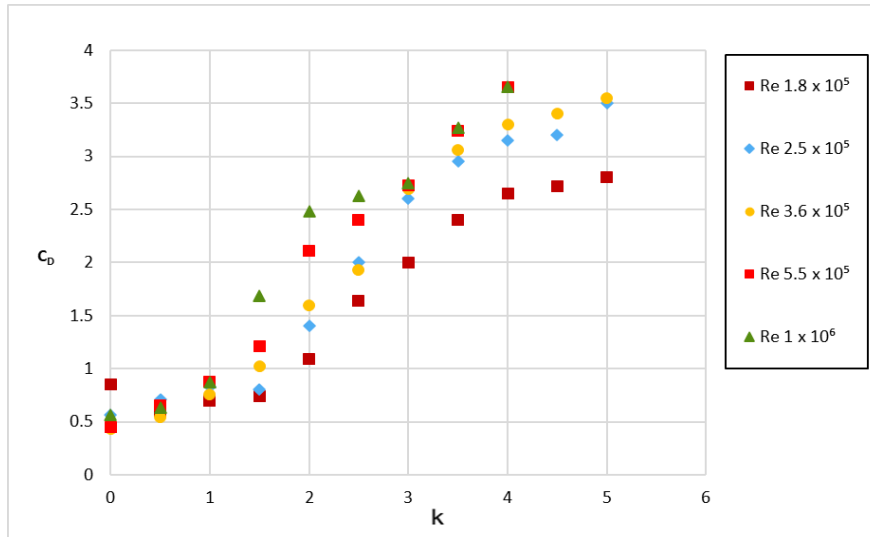


Fig. 7 Overall drag co-efficient versus spin ratio

The findings of [12], for a cylinder with two non-spinning endplates demonstrate that the slope of the coefficient of drag curve declines at  $k = 3$  but the slope does not become constant up to  $k = 5$  (Fig. 8). The results of this study show a comparable tendency with the results of [12], for a cylinder with non-spinning endplates. The differences in coefficient of drag found out in this study and the one done by [12], and [19], possibly, are due to the unlike Reynolds numbers used.

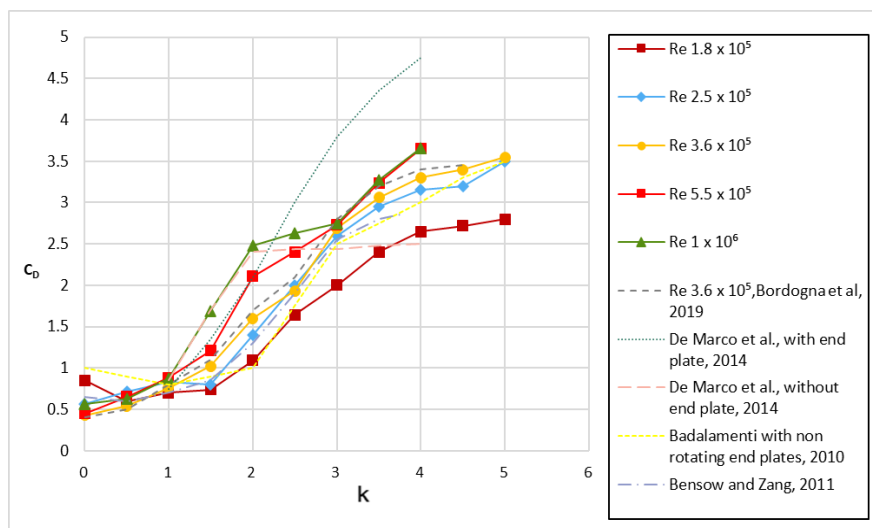
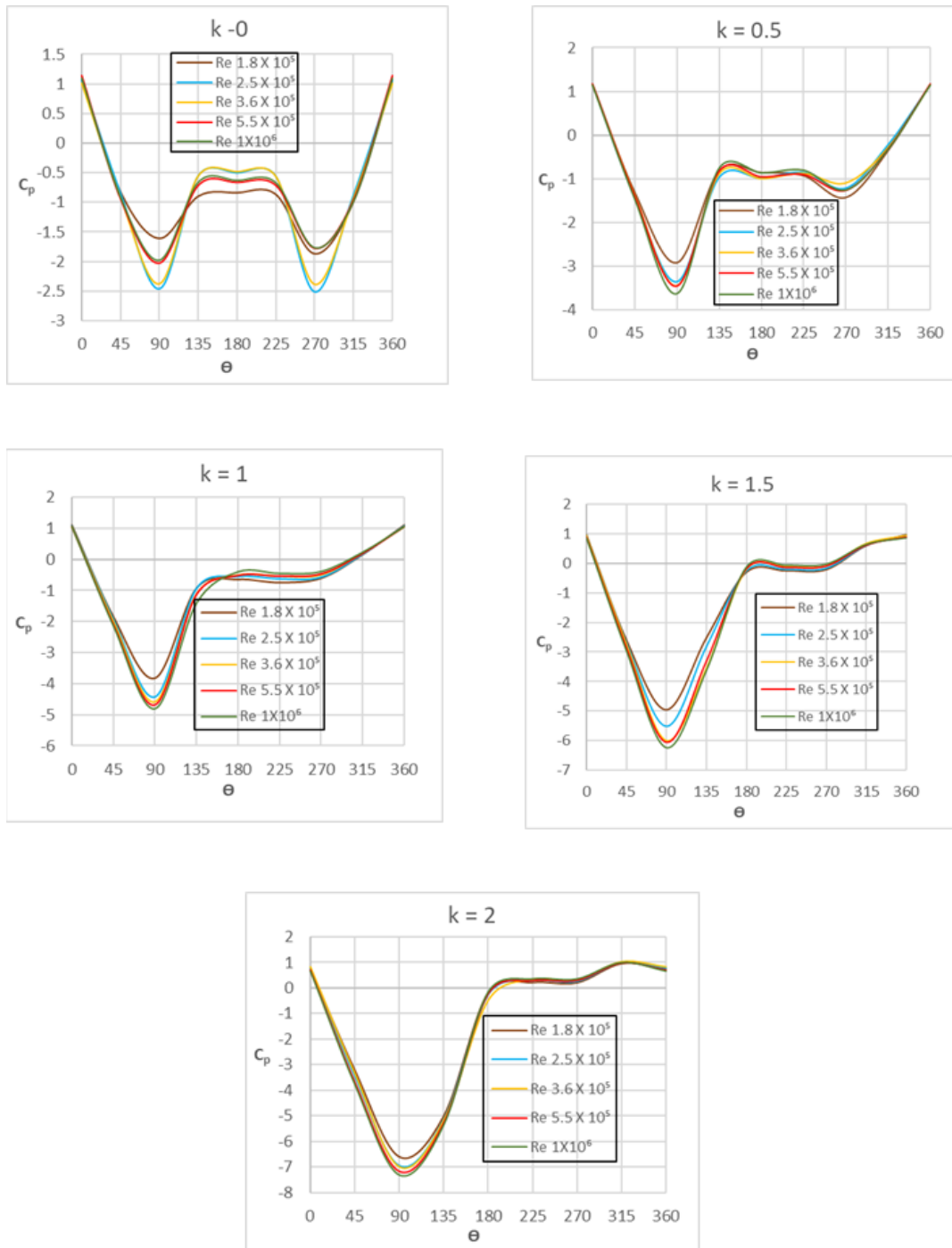


Fig. 8 Comparison drag coefficient with other studies

### C. PRESSURE COEFFICIENT

Fig. 9 and 10 show the pressure distribution around the cylinder.  $0^\circ$  points straight into the wind flow, while  $180^\circ$  is located on the cylinder away from the wind. The sectional coefficient of pressure  $C_p$  results support the results of coefficients of lift and drag observed in this study. The spinning of the cylinder is the reason for an asymmetry in the distribution of pressure on the sides of the Flettner rotor. This asymmetrical distribution of pressure results in the engendering of lift. For the spin ratio between 0.5 and 2, (Fig. 9), it is observed that higher the Reynolds number, higher will be the  $C_{pmin}$  and concurrently lower will be the  $C_{pmax}$ .

When the spin ratio is greater than 2.5, the  $C_p$  curves of the Reynolds numbers  $2.5 \times 10^5$  and  $3.6 \times 10^5$  almost overlap, (Fig. 10), this leads to comparable coefficients of lift and drag. In the spin ratio range between 1 and 2.5, the increase in the coefficient of drag at higher Reynolds numbers is triggered as the suction peak and the separation point shift to the rear end of the cylinder.



**Fig. 9 Pressure coefficients at mid-cylinder height for spin ratio  $k \leq 2$**

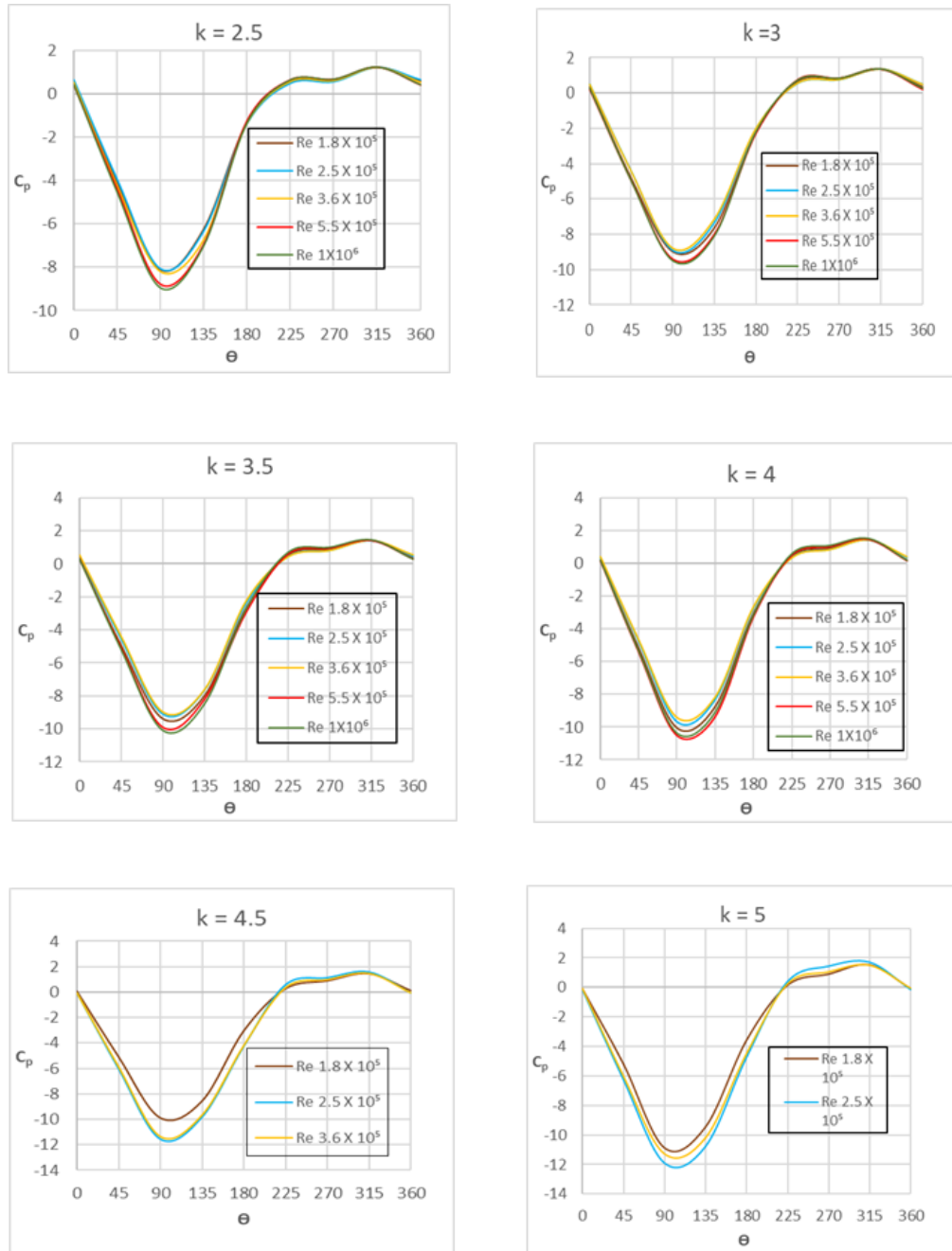


Fig. 10 Pressure coefficients at mid-cylinder height for spin ratio  $k > 2$

#### IV. CONCLUSION

This study aims at identifying the usefulness and industrial worth of Flettner rotor and studying the effect of the Reynolds number and spin ratio on the aerodynamic performance. For the considered range and spin ratio less than 2.5, the results show that, there is a noticeable impact of the Reynolds number on the coefficients of lift and drag. The coefficient of lift is affected by the Reynolds number in the critical flow region, but in the supercritical flow region the effect of Reynolds number is negligible. As the spin ratio increases, effect of the Reynolds number on the coefficient of lift reduces. However,



the Reynolds number influences the coefficient of drag for all flow conditions examined. It is observed that for spin ratios till  $k = 2.5$ , as the Reynolds number increases the lift and drag coefficients also increase. But, for spin ratios greater than 2.5, it is seen that the effect of the Reynolds number on the coefficient of lift is restricted. At spin ratio,  $k = 2$ , the coefficient of drag is highly affected by the different Reynolds numbers studied. The findings of this study have been juxtaposed with data available in similar published studies. In spite of the differences produced by the considerably different Reynolds numbers used, a good similarity is found with the results of [12], for Flettner rotor employing two non-rotating endplates. The results are also in agreement with the findings of [14], as similar aspect ratio and Reynolds number have been used in this study.

### REFERENCES

- [1] I.M.O., "Third IMO GHG study 2014," International Maritime Organization, London, 2015.
- [2] A. Schmidt, "E-Ship 1 - A wind-hybrid commercial cargo ship," September 2013. [Online]. Available: <https://www.stg-online.org/onTEAM/shipefficiency/programm/06-Andreas-Schmidt.pdf>. [Accessed January 2020].
- [3] E. Reid, "Test of rotating cylinders," NACA, Hampton, Virginia, 1924.
- [4] L. Prandtl, "Application of the "Magnus Effect" to the wind propulsion of ships," NACA, Hampton, Virginia, 1925.
- [5] F. Rizzo, "The Flettner rotor ship in the light of Kutta-Joukowski theory and of experimental results," NACA, Hampton, Virginia, 1925.
- [6] A. Thom, "Effect of discs on the air forces on a rotating cylinder," Aeronautical Research Committee, London, 1934.
- [7] W. Swanson, "The Magnus effect: A summary of investigations to date," vol. 83, no. 3, pp. 461-470, 1961.
- [8] B. Clayton, "BWEA Initiative on wind assisted ship propulsion (WASP)," in *Proceedings of the International Symposium on Windship Technology (WINDTECH '85)*, Southampton, 1985.
- [9] K. C. Morisseau, "Marine application of Magnus effect devices," vol. 97, pp. 51-57, 1985.
- [10] P. T. Tokumaru and P. E. Dimotakis, "The lift of a cylinder executing rotary motions in a uniform flow," *J. Fluid Mech.*, vol. 255, pp. 1-10, 1993.
- [11] C. Badalamenti and S. Prince, "Effects of endplates on a rotating cylinder in crossflow," in *Applied Aerodynamics Conference*, Honolulu, Hawaii, 2008.
- [12] C. Badalamenti, "On the Application of Rotating Cylinders to Micro Air Vehicles," City University, London, 2010.
- [13] W. Zhang, R. Bensow, V. Chernoray and M. Golubev, "Flow past a rotating finite length cylinder: numerical and experimental study," in *51st AIAA Aerospace Sciences Meeting including the New Horizons Forum and Aerospace Exposition*, Grapevine, Texas, 2013.
- [14] G. Bordogna, S. Muggiasca, S. Giappino, M. Belloli, J. Keuning, R. Huijsmans and A. v. ' . Veer, "Experiments on a Flettner rotor at critical and supercritical Reynolds numbers," *Journal of Wind Engineering & Industrial Aerodynamics*, vol. 188, pp. 19-29, 2019.
- [15] H. Badr, S. Dennis and P. Young, "Steady and unsteady flow past a rotating circular cylinder at low Reynolds numbers," *J. of Fluid Mechanics*, vol. 17, no. 4, pp. 579-609, 1989.
- [16] Y. Chew, M. Cheng and S. Luo, "A numerical study of flow past a rotating circular cylinder using a hybrid vortex scheme," Vols. 229, 35-71, 1995.
- [17] S. Mittal and B. Kumar, "Flow past a rotating cylinder," vol. 476, pp. 303-334, 2003.
- [18] S. Karabelas, "Large Eddy Simulation of high-Reynolds number flow past a rotating cylinder," vol. 31, pp. 518-527, 2010.
- [19] R. Bensow and W. Zhang, "Numerical simulation of high-Reynolds number flow around Flettner rotors," Southampton, 2011.
- [20] N. Thouault, N. Breitsamter, J. Seifert, C., Badalamenti and S. Prince, "Numerical analysis of a rotating cylinder with spanwise discs," Nice, France, 2010.
- [21] S. Karabelas, B.C.Koumroglou, C.D.Argyropoulos and N.C.Markatos, "High Reynolds number turbulent flow past a rotating cylinder," vol. 36, no. 1, pp. 379-398, 2012.
- [22] M. Everts, R. Ebrahim, E. Miles, M. Sharifpur, J. P. Meyer and J. Kruger, "Turbulent flow across a rotating cylinder with surface roughness," in *10th International conference on heat transfer, fluid mechanics and thermodynamics*, Florida, 2014.
- [23] A. De Marco, S.Mancini and C.Pensa, "Preliminary analysis for marine application of Flettner rotors," in *International Symposium on Naval Architecture and Maritime*, Yildiz Technical University, Istanbul, 2014.
- [24] M. Traut, P. Gilbert, C. Walsh, A. Bows, A. Filippone, P. Stansby and R. Wood, "Propulsive power contribution of a kite and a flettner rotor on selected shipping routes," *Applied Energy*, vol. 113, pp. 362-372, 2014.
- [25] F. Menter, "Two-equation Eddy-Viscosity turbulence models for engineering applications," vol. 32, no. 8, pp. 1598-1605, 1994.
- [26] A. De Marco, S.Mancini, C.Pensa, G.Calise and F.DeLuca, "Flettner Rotor Concept for Marine Applications: A Systematic Study," vol. Article ID 3458750, 2016.
- [27] D. Li, Leer-Andersen and A. B. M., "Performance and vortex formation of Flettner rotors at high Reynolds numbers," Gothenburg, Sweden, 2012.